

Butterfly Diradical Intermediates in Photochemical Reactions of $\text{Fe}_2(\text{CO})_6(\mu\text{-S}_2)$

Ioan Silaghi-Dumitrescu,^{*,§} Thomas E. Bitterwolf,^{*,†} and R. Bruce King^{*,‡}

Faculty of Chemistry and Chemical Engineering, Babeş-Bolyai University, Cluj-Napoca, Romania, Department of Chemistry, University of Idaho, Moscow, Idaho, and Department of Chemistry and Center for Computational Chemistry, University of Georgia, Athens, Georgia 30606

Received February 22, 2006; E-mail: rbking@chem.uga.edu

One of the most interesting recent developments in inorganic main group chemistry has been the discovery of singlet diradicals that are stable under ambient conditions,¹ including $(\text{R}_2\text{PBR}')_2$ (Figure 1),² $(\text{RPCR}')_2$, and $(\text{RNGeR}')_2$ structures,^{3,4} all with four-membered A_2B_2 rings. This communication reports the first evidence for similar diradical structures in transition metal carbonyl chemistry.

The iron carbonyl sulfide,⁵ $\text{Fe}_2(\text{CO})_6(\mu\text{-S}_2)$ (**I**), has become a very useful synthon in metal carbonyl chemistry⁶ as well as a model for the Fe-only hydrogenase from *C. pasteurianum*.⁷ X-ray diffraction indicates $\text{Fe}_2(\text{CO})_6(\mu\text{-S}_2)$ to have the tetrahedrane structure (Figure 2) with Fe–Fe and S–S bond distances of 2.55 and 2.01 Å, respectively. Photolysis of $\text{Fe}_2(\text{CO})_6(\mu\text{-S}_2)$ into the low-energy $d\sigma^*$ metal–ligand charge-transfer band at about 450 nm in the absence of potential ligands⁸ cleanly forms the cubane cluster⁹ $\text{Fe}_4(\text{CO})_{12}\text{S}_4$. Theoretical models¹⁰ indicate that the highest occupied molecular orbital (HOMO) of $\text{Fe}_2(\text{CO})_6(\mu\text{-S}_2)$ is dominantly Fe–Fe σ -bonding, whereas the lowest unoccupied molecular orbital (LUMO) is dominated by a σ^* S–S orbital. Excitation from the HOMO to the LUMO is thus predicted to have the unique property of simultaneously weakening both the Fe–Fe and S–S bonds.

We have now found that photolysis of $\text{Fe}_2(\text{CO})_6(\mu\text{-S}_2)$ at 450 ± 35 nm in a Nujol matrix¹¹ results in decrease of its strong $\nu(\text{CO})$ frequencies at 2040 and 2003 cm^{-1} and growth of product bands at 2091 (w), 2055 (s), 2033 (s), 2025 (s), and 1993 (w) cm^{-1} (Figure 3a). Careful repeated experiments established that no CO is lost in this photoreaction. Annealing the sample to ~ 140 K regenerated $\text{Fe}_2(\text{CO})_6(\mu\text{-S}_2)$. Photolysis of $\text{Fe}_2(\text{CO})_6(\mu\text{-S}_2)$ under ^{13}C at these wavelengths gave no measurable CO exchange. These observations indicate that this photoproduct is an isomer of $\text{Fe}_2(\text{CO})_6\text{S}_2$.

Photolysis of $\text{Fe}_2(\text{CO})_6(\mu\text{-S}_2)$ at lower wavelengths ($285 < \lambda_{\text{irr}} < 420$ nm) and thus higher energies generated a different set of new $\nu(\text{CO})$ frequencies at 2131(w), 2065(m), 2048(m), 2024(s), and 1995(m) cm^{-1} (Figure 3b). The band at 2131 cm^{-1} corresponds to free CO, indicating that formation of this product involves CO loss from $\text{Fe}_2(\text{CO})_6(\mu\text{-S}_2)$.

The stable tetrahedrane isomer of $\text{Fe}_2(\text{CO})_6(\mu\text{-S}_2)$ can be converted to two different butterfly isomers or a rhombus isomer by breaking one or both of the Fe–Fe and S–S bonds (Figure 4). Furthermore, structures for the two butterfly isomers of $\text{Fe}_2(\text{CO})_6\text{S}_2$ cannot be drawn without single electrons on either the pair of sulfur atoms (the Fe–Fe butterfly isomer) or on the pair of iron atoms (the S–S butterfly isomer). Therefore, each butterfly isomer of $\text{Fe}_2(\text{CO})_6\text{S}_2$ must be considered to be a diradical, as indicated in Figure 4.

The optimized geometries of these $\text{Fe}_2(\text{CO})_6\text{S}_2$ isomers, their relative energies, and their $\nu(\text{CO})$ vibrational frequencies have been

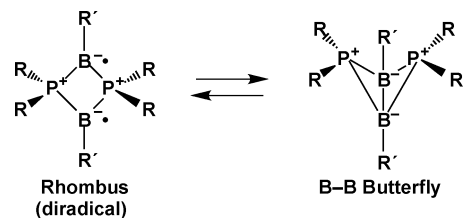


Figure 1. The Bertrand P_2B_2 diradical system (e.g., $\text{R} = i\text{-Pr}$ and $\text{R}' = t\text{-Bu}$).

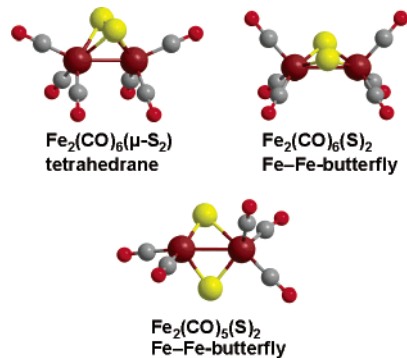


Figure 2. Structures for $\text{Fe}_2(\text{CO})_6\text{S}_2$ and $\text{Fe}_2(\text{CO})_5\text{S}_2$ discussed in this paper.

determined by density functional theory (DFT) methods using the BP86 functional with both the 6-311G(d) and lanl2dz basis sets (Table 1). In all cases, the optimized triplet isomers had higher energies than the corresponding singlet isomers and thus are not considered further in this communication.

The lowest energy $\text{Fe}_2(\text{CO})_6\text{S}_2$ isomer is the singlet tetrahedrane isomer (Figure 2). Its calculated Fe–Fe and S–S distances match very close to the experimental values noted above. Next in energy at +13.6 kcal/mol is the singlet Fe–Fe butterfly isomer formed by breaking the S–S bond in the tetrahedrane structure but retaining the Fe–Fe bond as the “body” of the butterfly (Figure 2b). The singlet rhombus isomer of $\text{Fe}_2(\text{CO})_6\text{S}_2$ without a direct Fe–Fe or S–S bond (Figure 4) lies at a still higher energy of +29.8 kcal/mol and corresponds to the transition state for the Fe–Fe butterfly flapping its Fe_2S “wings.” The singlet S–S butterfly lies at the highest energy (39.3 kcal/mol) of the four singlet $\text{Fe}_2(\text{CO})_6\text{S}_2$ isomers considered in this communication.

The calculated $\nu(\text{CO})$ frequencies for the $\text{Fe}_2(\text{CO})_6(\mu\text{-S}_2)$ tetrahedrane (Figure 2) match very closely to the experimental values (Table 2). More interestingly, the observed $\nu(\text{CO})$ frequencies for the isomer of $\text{Fe}_2(\text{CO})_6\text{S}_2$ generated in the low-temperature Nujol matrix by photolysis at 450 ± 35 nm (Table 2) are very close to those calculated for the singlet Fe–Fe butterfly isomer (Figure 2). In addition, the observed $\nu(\text{CO})$ frequencies for the isomer of $\text{Fe}_2(\text{CO})_6\text{S}_2$ generated in Nujol by photolysis at higher energies (420–

[§] Babeş-Bolyai University.

[†] University of Idaho.

[‡] University of Georgia.

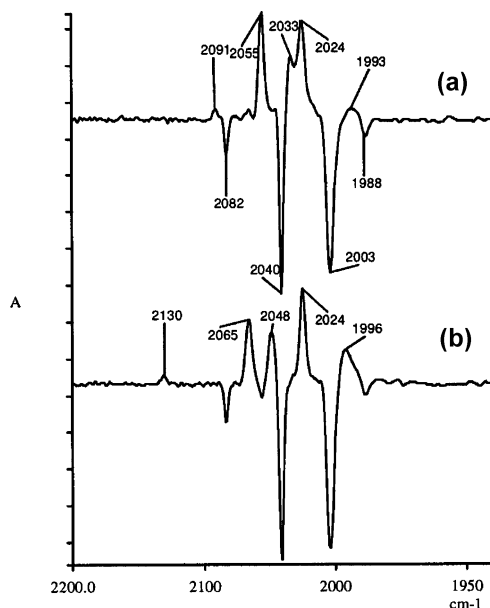


Figure 3. Nujol matrix photolysis of $\text{Fe}_2(\text{CO})_6(\mu\text{-S})_2$: (a) 30 min photolysis at $\lambda_{\text{irr}} = 450 \pm 35$ nm minus starting material; (b) 30 min photolysis at $285 \text{ nm} < \lambda_{\text{irr}} < 420$ nm.

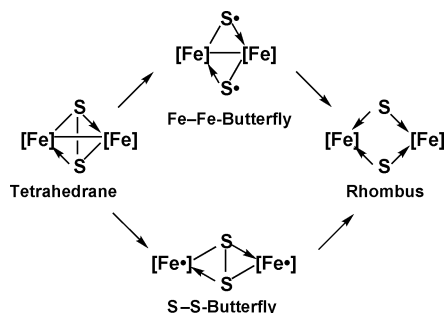


Figure 4. The isomers of $\text{Fe}_2(\text{CO})_6(\mu\text{-S})_2$ ([Fe] = $\text{Fe}(\text{CO})_3$) showing the single electrons in the Fe–Fe butterfly and S–S butterfly diradical structures.

Table 1. The Four Singlet Isomers of $\text{Fe}_2(\text{CO})_6\text{S}_2$ (Figure 2) Listed in Order of Increasing Energy^a

$\text{Fe}_2(\text{CO})_6\text{S}_2$ isomer	relative energy kcal/mol	Fe–Fe Å	S–S Å	imaginary frequencies
tetrahedrane	0.0	2.503	2.083	none
Fe–Fe butterfly	13.6	2.746	3.139	none
rhombus	29.8	3.375	2.957	$69i \text{ cm}^{-1}$
S–S butterfly	39.3	3.645	2.160	$35i \text{ cm}^{-1}$

^a These calculations were performed using the BP86 method with the 6-311G(d) basis set. Only singlet isomers are considered here. The relative energies of these isomers were similar using the lan12dz basis set rather than the 6-311G* basis set.

280 nm) are very close to those calculated for the optimized $\text{Fe}_2(\text{CO})_5\text{S}_2$ product formed by loss of CO from the Fe–Fe butterfly isomer (Table 2 and Figure 2). These observations and the small singlet–triplet energy separation^{1d} of 9.7 kcal/mol provide compelling evidence that the iron carbonyl sulfides generated upon photolysis of the $\text{Fe}_2(\text{CO})_6(\mu\text{-S})_2$ tetrahedrane have singlet diradical structures with an Fe–Fe butterfly structure of the central Fe_2S_2 unit. The coexistence of the $\text{Fe}_2(\text{CO})_6\text{S}_2$ tetrahedrane and Fe–Fe butterfly isomers observed in solution in this work is related to the

Table 2. A Comparison of Experimental and Calculated $\nu(\text{CO})$ Frequencies for Selected $\text{Fe}_2(\text{CO})_6\text{S}_2$ Isomers

$\text{Fe}_2(\text{CO})_6\text{S}_2$ isomer		$\nu(\text{CO})$ frequencies, cm^{-1} (relative infrared intensities of calcd frequencies in parentheses)
tetrahedrane	calcd	2075(260), 2039(1530), 2010(1220), 2005(760), 1989(140)
tetrahedrane	expt	2082(m), 2040(s), 2003(s), 1988(w)
Fe–Fe butterfly	calcd	2082(53), 2056(1760), 2023(1470), 2023(990), 2014(2)
photolysis product at 450 ± 35 nm	expt	2090(w), 2055(s), 2034(m), 2025(s), 1993(w)
Fe–Fe butterfly for $\text{Fe}_2(\text{CO})_5\text{S}_2$	calcd	2065(340), 2027(1780), 2020(648), 2013(724), 1992(496)
photolysis product at 280–420 nm	expt	2131(w), 2065(m), 2048(m), 2024(s), 1995(m)

coexistence of singlet diradical and bicyclobutane isomers of (*i*-Pr₂PBPh)₂ in solution observed by Bertrand and co-workers.^{2d}

The tetrahedrane $\text{Fe}_2(\text{CO})_6(\mu\text{-S})_2$ is known to undergo [2 + 2] cycloadditions with concurrent rupture of the S–S bond with a variety of substrates, including alkenes,¹² alkynes,¹³ and even fullerenes¹⁴ as well as photochemical insertion of CO into the S–S bond.¹⁵ The work presented in this communication provides compelling evidence that such reactions proceed through Fe–Fe butterfly diradical $\text{Fe}_2(\text{CO})_6\text{S}_2$ intermediates.

Acknowledgment. We are indebted to the National Science Foundation for support of this work under Grants CHE-0209857 and CHE-0315226. Part of this work was undertaken with the financial support from CNCSIS-Roumania.

Supporting Information Available: Calculated energies and bond lengths in $\text{Fe}_2(\text{CO})_6\text{S}_2$ clusters; Cartesian coordinates and figures of all of the optimized structures. This material is available free of charge via the Internet at <http://pubs.acs.org>.

References

- Grützmaier, H.; Breher, F. *Angew. Chem., Int. Ed.* **2002**, *41*, 4006.
- (a) Scheschke, D.; Amii, H.; Gornitzka, H.; Schoeller, W. W.; Bourissou, D.; Bertrand, G. *Science* **2002**, *295*, 1880. (b) Scheschke, D.; Amii, H.; Gornitzka, H.; Schoeller, W. W.; Bourissou, D.; Bertrand, G. *Angew. Chem., Int. Ed.* **2004**, *43*, 585. (c) Amii, H.; Vranicar, L.; Gornitzka, H.; Bourissou, D.; Bertrand, G. *J. Am. Chem. Soc.* **2004**, *126*, 1344. (d) Rodriguez, A.; Olsen, R. A.; Ghaderi, N.; Scheschke, D.; Tham, F. S.; Mueller, L. J.; Bertrand, G.; Cheng, M.-J.; Hu, C.-N. *Mol. Phys.* **2003**, *101*, 1319.
- Sebastian, M.; Nieger, M.; Szieberth, D.; Nyulász, L.; Niecke, E. *Angew. Chem., Int. Ed.* **2004**, *43*, 637.
- Cui, C.; Brynda, M.; Olmstead, M. M.; Power, P. P. *J. Am. Chem. Soc.* **2004**, *126*, 6510.
- Hieber, W.; Gruber, J. Z. *Anorg. Allg. Chem.* **1958**, *296*, 91.
- King, R. B.; Bitterwolf, T. E. *Coord. Chem. Rev.* **2000**, *206–207*, 563.
- Peters, J. W.; Lanzilotta, W. N.; Lemon, B. J.; Seefeldt, L. C. *Science* **1998**, *282*, 1853.
- Kunkely, H.; Vogler, A. J. *Organomet. Chem.* **1998**, *568*, 291.
- Bogan, L. E.; Lesch, D. A.; Rauchfuss, T. B. *J. Organomet. Chem.* **1983**, *568*, 291.
- DeKock, R. L.; Baerends, E. J.; Hengelmolen, R. *Organometallics* **1984**, *3*, 289.
- Bitterwolf, T. E.; Lott, K. A.; Rest, A. J.; Mascetti, J. J. *Organomet. Chem.* **1991**, *419*, 113.
- Kramer, A.; Lorenz, I. P. *J. Organomet. Chem.* **1990**, *388*, 187 and references therein.
- Seyferth, D.; Henderson, R. S. *J. Organomet. Chem.* **1991**, *419*, 113.
- Westmeyer, M. D.; Galloway, C. P.; Rauchfuss, T. B. *Inorg. Chem.* **1994**, *33*, 4615.
- Messelhäuser, J.; Gutenson, K. U.; Lorenz, I.-P.; Hiller, W. *J. Organomet. Chem.* **1987**, *321*, 377.

JA061272Q